



Mechanisms of oxidative stress caused by CuO nanoparticles to membranes of the bacterium *Streptomyces coelicolor* M145



Xiaomei Liu^a, Jingchun Tang^{a,*}, Lan Wang^a, John P. Giesy^{b,c}

^a Key Laboratory of Pollution Processes and Environmental Criteria (Ministry of Education), Tianjin Engineering Research Center of Environmental Diagnosis and Contamination Remediation, College of Environmental Science and Engineering, Nankai University, Tianjin 300350, China

^b Toxicology Centre, University of Saskatchewan, Saskatoon, Saskatchewan, Canada

^c Department of Veterinary Biomedical Sciences, University of Saskatchewan, Saskatoon, Saskatchewan, Canada

ARTICLE INFO

Keywords:

CuO NPs

Streptomyces coelicolor M145

Viability assay

CLSM

ROS

ABSTRACT

Toxic effects of widely used CuO nanoparticles (NPs) on the genus *Streptomyces* has been seldom studied. This work investigated toxicities of several sizes of CuO nanoparticles (NPs) to *Streptomyces coelicolor* M145 (*S. coelicolor* M145). Compared with NPs, toxicity of micrometer-sized CuO on M145 was trivial. In 0.9% NaCl, when the concentration of CuO NPs was 100 mg/L, survival of bacteria increased from 18.3% in 20 nm particles to 31.1% in 100 nm particles. With increasing concentrations of CuO, the level of ROS gradually increased and there were significant differences ($p < 0.05$) in ROS exposed to 20, 40 and 100 nm (80 nm) CuO NPs. In TSBY medium, toxicity of CuO NPs was less and mainly attributed to release of Cu^{2+} , analysis by confocal laser scanning microscope (CLSM) showed that size of the mycelium did not change although some individual bacteria died. This was likely due to Cu^{2+} released from NPs entering cells through the membrane, while in 0.9% NaCl, lesions on membranes was caused by NPs outside the bacteria. This research indicated that toxicity of CuO NPs to *S. coelicolor*, is related to both size of NPs and is dependent on characteristics of the medium.

Capsule: This is the first time to measure the toxicity of nano materials to *Streptomyces*, and toxic CuO NPs to *Streptomyces* have been shown to differ depending on medium.

1. Introduction

NPs are materials ranging in size from 1 nm to 100 nm in at least one dimension (Dinesh et al., 2012). Due to their unique antimicrobial, electronic, optical, and structural strength enhancement properties, today NPs are used in virtually all fields (Balazs et al., 2006; Lee et al., 2010). An inventory of NP-enabled products, which mainly includes metals and metal oxides, applications indicates that more than 1814 products are being manufactured and the number is projected to triple by 2020 (Robichaud et al., 2009; Vance et al., 2015; Woodrow Wilson Database). Among them, CuO NPs is one of the most common NPs used in industry. Compared with bulk particle CuO (CuO BP), CuO NPs exhibit unique physical and chemical properties, so that it has been successfully used in many fields, such as electronic equipment, sensors, superconducting materials and thermal conductivity materials (Aprile et al., 2010; Ben-Moshe et al., 2009). In addition, because of its antibacterial ability, it can be used as a novel plastic antimicrobial agent and is widely used in breeding of livestock and poultry (Delgado et al.,

2011).

The increasing usage of CuO NPs in industry, agricultural applications, consumer products and a variety of medical applications, inevitably leads to releases of CuO NPs into the environment. Currently, due to the potential risks to ecological systems, these releases have become an emerging issue (Eduok et al., 2013; Schaumann et al., 2015). As an important part of ecosystems, toxic effects of NPs on bacteria had aroused extensive attention. It had been confirmed that CuO NPs can inhibit many kinds of bacteria, such as *Vibrio fischeri* (Heinlaan et al., 2008), *Escherichia coli* (*E. coli*), *Bacillus subtilis*, *Streptococcus aureus* (Baek and An, 2011). However, studies of a unique bacterium-*Streptomyces* have been rare. *Streptomyces* is a high genome G + C, gram-positive, filamentous bacterium that can generate various industrially important secondary metabolites (Borodina et al., 2008), two of which are pigmented: a diffusible blue pigmented actinorhodin and undecylprodigiosin (cell wall associated, red pigment) (Kim et al., 2016). Actinorhodin is a weak antibiotic, while undecylprodigiosin on the other hand, is known to have antimicrobial activities,

Abbreviations: NPs, nanoparticles; *S. coelicolor*, *Streptomyces coelicolor*; CLSM, confocal laser scanning microscope; BP, bulk particle; h, hours; *E. coli*, *Escherichia coli*; DLS, Dynamic Light Scattering; MS, mannitol soy; PI, propidium iodide; SEM, scanning electron microscope

* Corresponding author.

E-mail address: tangjch@nankai.edu.cn (J. Tang).

<https://doi.org/10.1016/j.ecoenv.2018.04.007>

Received 1 February 2018; Received in revised form 3 April 2018; Accepted 4 April 2018
0147-6513/© 2018 Elsevier Inc. All rights reserved.

immunosuppressive and anticancer properties (Williamson et al., 2006). *Streptomyces* have complex life cycles, undergoing differentiation from spore to substrate hyphae, aerial hyphae, spore chains, and mature spore (Bentley et al., 2002). Meanwhile, morphological differentiation of *Streptomyces* is generally sensitive to environmental stresses, such as heat, osmotic pressure and nutrients (Bibb, 2005). Therefore, *Streptomyces* can be an ideal model to study responses of microbes to NPs. However, the toxic effects of NPs to *Streptomyces* had been little studied and described.

Toxicity of CuO NPs has been studied and much debate still exists about the mechanisms of toxicity of CuO NPs. Results of recent studies indicated that oxidative stress and dissolved ions played important roles in toxicities of NPs (Jin et al., 2010; Horie et al., 2012; Napierska et al., 2012). Integrities of membranes was a primary indicator of effects of NPs on bacteria under adverse stress (Kang et al., 2008). Results of some studies suggested that CuO NPs functioned via the specific particle effects. After 2 h (hours) exposure, inhibition of 45.4% was observed on *E. coli* at 10 mg/L of CuO NPs, but the dissolved Cu²⁺ ions at this concentration had no obvious toxicity (0.83% inhibition) (Zhao et al., 2013). In another study using different bacteria, it appeared that particles played principal role in toxicity while that of copper ions was negligible (Baek and An, 2011). However, some researchers insisted that from a toxicology perspective, dissolved copper was more harmful to organisms than solid copper particles (Aruoja et al., 2009). Therefore, when studying toxicity of CuO NPs to microbes determining whether particles or released ions are responsible for toxicity. This is important for determining doses and affects of accessory factors on toxic potencies of CuO NPs. In addition, media used by various researchers were not the same. Some media were inorganic (Jin et al., 2010) while others contained mixtures of organic substances (Napierska et al., 2012) and some used water collected from natural environments (Tong et al., 2013). Results of several studies have shown that solubility of CuO NPs in solution was affected by organic matters (Gunawan et al., 2011; Zhao et al., 2013). Therefore, in order to verify whether the medium could affect the toxicity of CuO to *Streptomyces*, in this experiment, two typical medium, 0.9% NaCl and an organic rich medium- TSBY were used.

Toxicity to *S. coelicolor* M145 was determined and the mechanism was explored during exposure to CuO either in the form of NPs or BPs in each of two culture media, 0.9% NaCl or organic rich TSBY. To our knowledge, it was the first holistic investigation on the toxicity of CuO NPs to *Streptomyces*.

2. Materials and methods

2.1. Characterization of CuO NPs

CuO NPs of 20, 40, 80 or 100 nm as well as BPs (1 μ m) were purchased from Shanghai Macklin Biochemical company (China). Sizes and morphologies of particles were evaluated by use of a JSM-7800 scanning electron microscop (SEM, JEOL, Japan) (Rajesh et al., 2012). CuO NPs and BPs suspensions (10, 20, 40, 100 mg/L) were prepared by adding dry particles into 0.9% NaCl or TSBY media (Trypticase Soy Broth: 30 g/L, Sucrose: 340 g/L, Yeast extract: 5 g/L) (Yang et al., 2012), then sonicated (100 W, 40 kHz) for 30 min and shaken for 2 h to facilitate dispersion. Sizes of particles and agglomerates in solution were measured by Dynamic Light Scattering (DLS) with a Zetasizer nano ZS (Malvern, UK). The pH and EC of the particle suspensions were then measured (Wang et al., 2009). Data were collected in triplicate at 25 °C.

2.2. Cultivation of bacterial

The organism used in this study was a unique, Gram-positive bacterium, *S. coelicolor* M145, purchased from China General Microbiological Culture Collection Center (Beijing, China). For spore

production, *S. coelicolor* was cultivated on mannitol soy (MS) agar plates for 7 days at 30 °C, and harvested by scraping and suspending in 20% (v/v) glycerol and stored at – 80 °C (Sigle et al., 2016). Seed culture of *S. coelicolor* was prepared by inoculating spores into a special shaking flask with 100 mL of TSBY liquid medium, and incubated at 30 °C with shaking at 150 rpm for 48 h. Germinated spores were harvested by centrifugation at 6000 \times g for 10 min (Bhatia et al., 2016).

To measure growth of *S. coelicolor* M145, triplicate samples of mycelium were washed three times with 0.9% NaCl and collected on a pre-weighed filter by vacuum. Filters with associated mycelium were freeze-dried and mass determined (Hesketh et al., 2007; Huang et al., 2015). The difference between the latter and the initial values was defined as the dry mass of bacteria.

2.3. Viability staining and confocal laser scanning microscope analysis

Cytotoxicity to *S. coelicolor* M145 was assessed by measuring changes of relative abundance of viable cells with the LIVE/DEAD Bac-Light bacterial viability kit (L-13152; Invitrogen). Cells were stained with two stains, propidium iodide (PI), a red fluorescent nucleic acid stain in order to detect dead cells and SYTO 9, a green fluorescent nucleic acid stain to detect the viable cells. SYTO 9 green fluorescent stain labels all of the cells no matter the membranes intact or damaged. In contrast, PI as a non-cell-permeating stain, labels only bacteria with damaged membranes. Thus, in the presence of both stains, bacteria with intact cell membranes appear fluorescent green whereas bacteria with damaged membranes appear red (Binh et al., 2014).

S. coelicolor M145 was cultured for 48 h in TSBY medium before measuring toxicity of CuO, and then the solution was centrifuged and washed with 0.9% NaCl three times. Series concentration of CuO NPs were first prepared with two different solutions – 0.9% NaCl and TSBY medium. Suspensions of 50 μ L were added to 96 well microplates with 3 replicates per treatment. Plates were incubated at 30 °C with shaking at 150 rpm on an orbital shaker (HNY-2102C, Honour, China). After 4 h of incubation, 50 μ L Bac-Light solution (SYTO 9: PI = 1:1) was added to each well and plates were incubated with shaking for 15 min in the dark. The green (excitation 485 nm and emission 530 nm) and red (excitation 485 nm and emission 630 nm) fluorescence of each well were measured by Microplate reader (synergy h4, BioTek). Relative abundances of viable bacterial cells in each well were expressed as a ratio of green to red fluorescence signals (live dead ratio). A calibration curve was obtained by using cultures of *S. coelicolor* M145 mixtures with known percentages of live and dead cells. The percentage of viable bacteria for different treatments was normalized by the calibration curve (Tong et al., 2013). After staining, samples were examined under a confocal laser scanning microscope (LSM880 with Airyscan, Zeiss, Germany) with the same wavelengths as the microplate reader.

2.4. Intracellular reactive oxygen species (ROS)

Concentrations of intracellular ROS in *S. coelicolor* M145 were determined by ROS Assay Kit (Beyotime, China). In the kit, a cell permeable 2',7'-dichlorofluorescein diacetate (DCFH-DA) is used as a oxidation-sensitive dye, which can be deacetylated by esterases into dichlorofluorescein (DCFH), and DCFH can't cross cell membranes freely. Finally DCFH is oxidized into fluorescent 2',7'-dichlorofluorescein (DCF) by intracellular ROS to indicate concentrations of intracellular ROS. Briefly, after 4 h exposure, the pellets were centrifuged and washed three times with 0.9% NaCl. Then suspended with 10 μ mol/L DCFH-DA and incubated in the dark at 30 °C for 30 min, followed by washing three times with 0.9% NaCl. Then 100 μ L solution was added to 96 well microplates. The fluorescence intensity was measured by microplate reader at an excitation wavelength of 485 nm and an emission wavelength of 530 nm. The relative ROS level was represented as the fluorescence intensity ratio of the exposure group to the control group with the same dry mass (Li et al., 2016).

2.5. Analysis of the concentration of Cu^{2+} in the medium and bacterial cell

To estimate dissolution of free Cu from CuO NPs into media, concentrations of Cu^{2+} were determined after shaking for 4 h. Suspensions were centrifuged at $10,000 \times g$ for 20 min (Wang et al., 2009). The supernatant was filtered twice by $0.22 \mu\text{m}$ Nylon membranes filters and Cu^{2+} was determined using a continuum source atomic absorption spectrometry (contraAA 700, Jena, German).

To quantify total concentrations of copper (Cu) in bacterial biomass, *S. coelicolor* M145 was cultured for 48 h in TSBY medium then cells separated from suspension by centrifugation and washed three times with 0.9% NaCl. A series of concentration of CuO NPs was prepared in 0.9% NaCl or TSBY media and bacteria incubated 4 h, at 30°C with shaking at 150 rpm on an orbital shaker. Then biomass was centrifuged and washed with 0.9% NaCl for 3 times and 0.25 g cell were weighed after freeze-drying. 4 mL HNO_3 and 2 mL H_2O_2 were used to digest cells in a microwave digestion system (MDS-15, Sineo, China) at 800 W, 120°C for 10 min and then 800 W, 160°C for 20 min. All digested samples were filtered through $0.22 \mu\text{m}$ Nylon membrane filters, and final volume was adjusted to 50 mL with distilled water (Mohmand et al., 2015). Finally Cu^{2+} was quantified by use of inductively coupled plasma with mass spectroscopy (Elan drc-e, Perkin Elmer, USA).

3. Results and discussion

3.1. Characterization of CuO NPs

Based on SEM images of various sizes of CuO NPs (Fig. 1) their diameters were consistent with those specified by the manufacturer. The size distributions in TSBY medium and 0.9% NaCl were measured by DLS analysis (Supplementary Table S1), which showed larger sizes than that measured by SEM as particles formed agglomerates in liquid media. In 0.9% NaCl, sizes of NPs ranged from 268 to 412 nm, while in TSBY medium, the range was 942–1034 nm. These results demonstrated that NPs formed larger aggregates in TSBY medium. The pH ranged from 6.29 to 6.76 in 0.9% NaCl, but in TSBY medium, pH of various particles was almost the same, ranging from 6.60 to 6.72.

Similarly, EC values were 6.97–13.42 $\mu\text{s}/\text{cm}$ in 0.9% NaCl, but 6.21–6.33 ms/cm in TSBY medium. In 0.9% NaCl solution, the increasing of pH with elevated concentration of NP was probably caused by hydrolysis of Cu^{2+} released from CuO NPs, while decreasing of EC value was caused by adsorption of NaCl by NPs.

3.2. The toxicity of different size of CuO particles to *S. coelicolor* M145

Effects of CuO NPs on growth of *S. coelicolor* M145 was investigated by measuring dry masses of cells in TSBY medium after 48 h. When same concentration of CuO 40 mg/L was chosen, similar growth curves were observed for the control and BP CuO, while growth was similarly inhibited by several sizes of CuO NPs (Supplementary Fig. S1). There was no significant difference between growth of *S. coelicolor* exposed to 20 or 100 nm CuO NPs.

In order to verify whether size affected toxicity of CuO to *S. coelicolor* M145, a series of CuO of varying size; 20, 40, 80 and 100 nm and $1 \mu\text{m}$, were checked in each of two media. The Bac-Light bacterial viability assay as a well-accepted criterion for characterizing viability of bacterial cells was employed to monitor membrane integrity (Chu et al., 2015). In this method, the survival rate of bacteria without CuO NPs was defined to be 100%. It showed that in the two media, there was difference in the relative abundance of viable bacteria of M145. In 0.9% NaCl (Fig. 2a), except for those exposed to 80 and 100 nm, there were significant differences ($p < 0.05$) in viability of cells exposed to each size of CuO NPs at concentrations of 40 and 100 mg/L concentration. When concentrations of various sizes of NPs were 100 mg/L, the viability of *S. coelicolor* M145 was 18–31% after 4 h-exposure. While in TSBY medium (Fig. 2b), viability was 70% in medium containing 100 mg/L NPs, and toxicity of CuO NPs of various sizes from 20 to 100 nm were almost the same. Compared with CuO NPs, the toxicity of BPs ($1 \mu\text{m}$) to *Streptomyces* was much less in both media.

ROS was directly proportional to concentrations of CuO NPs (Fig. 3). In 0.9% NaCl (Fig. 3a), there were significant differences ($p < 0.05$) in concentrations of ROS in cells exposed to 20, 40 or 100 nm (80 nm) CuO NPs at concentration of 10, 20, 40 or 100 mg/L, while there was no significant difference ($p > 0.05$) between ROS in

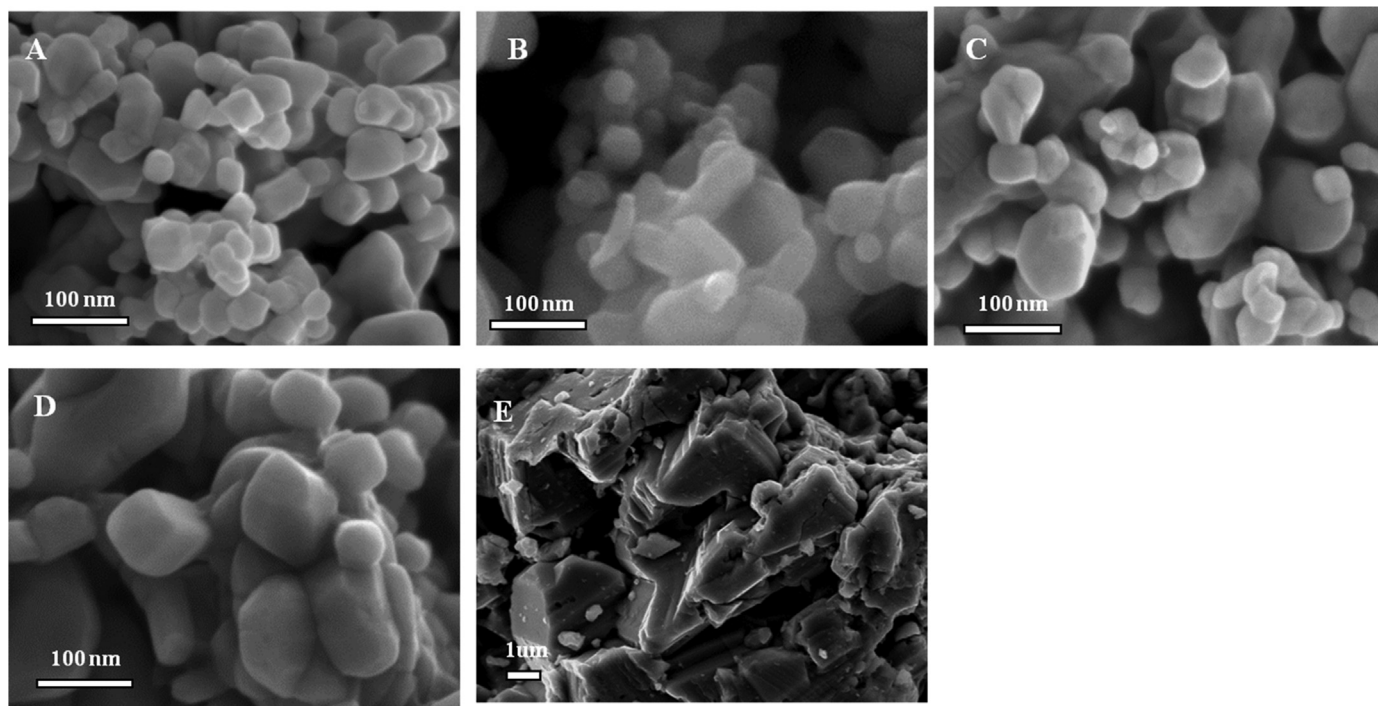


Fig. 1. SEM images of CuO particles with different size. a: 20 nm, b: 40 nm, c: 80 nm, d: 100 nm, e: $1 \mu\text{m}$.

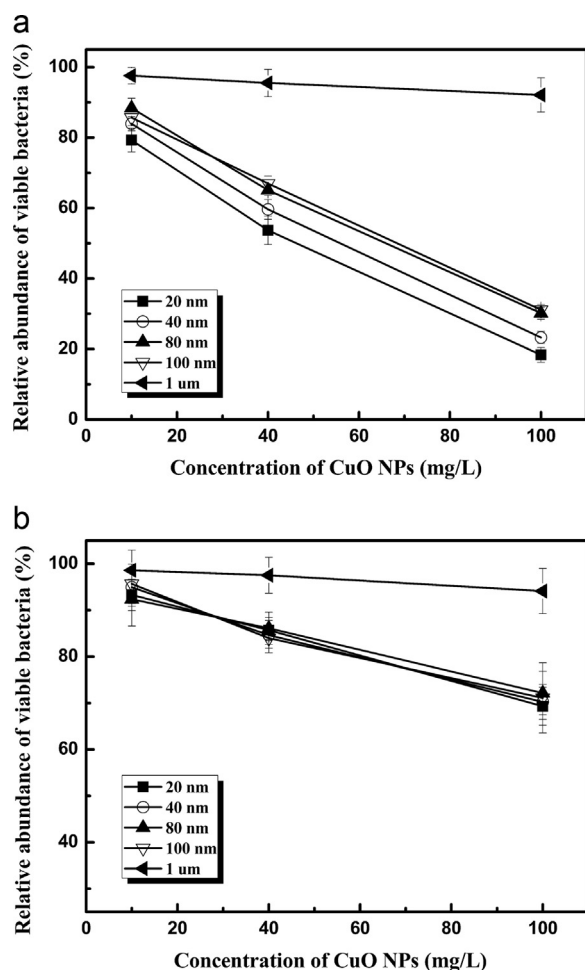


Fig. 2. Relative abundances of viable *S. coelicolor* M145 among treatments of different size and different concentration of CuO NPs in two media, (a) 0.9% NaCl, (b) TSBY medium. Error bar represent standard deviation ($n = 3$).

cells exposed to 80 or 100 nm CuO NPs. When exposure to 100 mg/L CuO NPs the concentration of ROS was 5–6 fold greater than that of control without CuO NPs exposure. In TSBY medium (Fig. 3b), the concentration of ROS level was less, and exposure to 100 mg/L resulted in a concentration of ROS that was 3.5–4 fold greater than that of the control. However, in TSBY medium, exposure to 10 mg/L CuO NPs did not result in higher concentrations of ROS than that in control cells or cells exposed to 1 μm CuO NPs. At concentrations of 20 or 40 mg/L, there were significant differences ($p < 0.05$) in concentrations of ROS in cells exposed to 20 nm CuO NPs and other sizes. Although in TSBY medium viabilities of cells exposed to these sizes of NP were almost the same, data on concentrations of ROS indicated that there was a difference in toxicity among sizes of CuO NPs. Combined with the subsequent results, it was concluded that in TSBY medium Cu^{2+} was more toxic than were CuO NPs and there were no significant differences in amount of Cu^{2+} that was ablated from the various sizes of CuO NPs. For that reason rates of viability were almost the same, regardless of the size. There were still a small amount of solid particles in present, which was the cause of significant differences in concentrations of ROS. For BPs (1 μm), the ROS exposed to concentration of 40 mg/L was approximately 1.4-fold that others in both types of media, which verified that toxicity of BPs to *Streptomyces* was weak.

When cells of *S. coelicolor* M145, exposed to various sizes of CuO NPs, were examined by confocal laser scanning microscopy in 0.9% NaCl (Fig. 4a), it was found that the size of mycelium pellets became smaller in treatments of 20–100 nm CuO NPs (0.11–0.18 mm) as compared to control (0.34 mm) or BP (0.32 mm) (Supplementary Table S2).

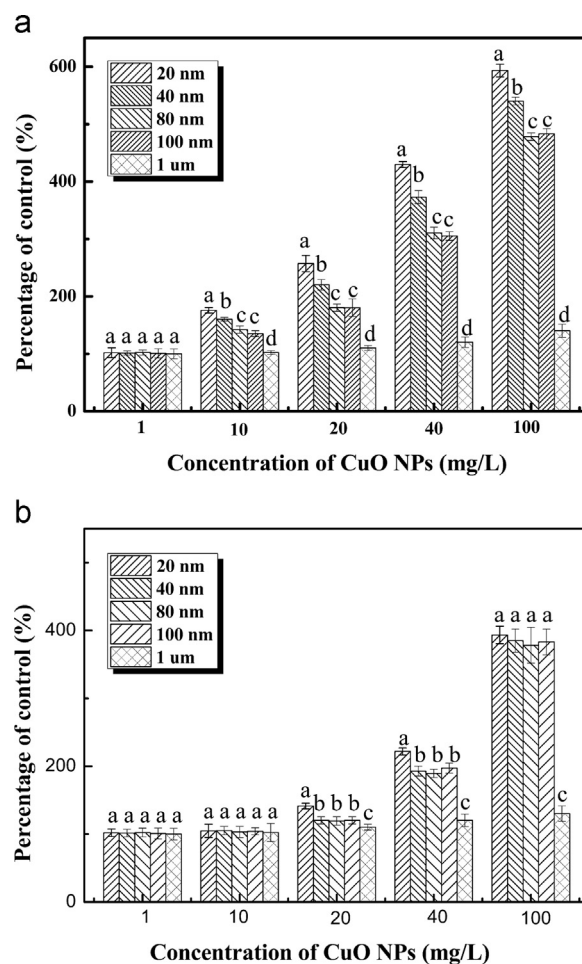


Fig. 3. Intracellular ROS levels of *S. coelicolor* M145 among treatments of different size and different concentration of CuO in two media: (a) 0.9% NaCl, (b) TSBY medium. Different letters indicates that the treatment was significantly different ($p < 0.05$) from others at the same concentration of CuO NPs. a, b, c indicates significant difference among different treatment. Error bar represent standard deviation ($n = 3$).

This result indicated that CuO NPs killed the bacteria by destroying the cell membrane, with hyphae broken, such that mycelia became smaller. In addition, the color of the PI stain became dominant at greater concentrations of CuO NPs, which meant the percentage of dead bacteria was greater. It can be concluded that larger size of CuO NPs exhibited lesser toxic potencies. While in TSBY medium (Fig. 4b), the size of mycelium pellets decreased from 0.34 mm to 0.26 mm (Supplementary Table S2) and the ratio of dead to live bacteria increased. This result indicated that CuO NPs killed the bacteria but didn't destroy cell membranes. Exposure of *S. coelicolor* to 100 mg/L BP CuO did not alter the phenotype from that observed in the control, which was in consistent with the above conclusions.

3.3. Mechanisms of toxic action of CuO NPs to *S. coelicolor* M145

In TSBY medium, the size of mycelium pellets was not proportional to treatment but the ratio of dead bacteria increased as a function of concentrations of CuO NPs (Fig. 4b). This result indicated that the cell membranes were not damaged because Cu^{2+} could enter the cell, while it was toxic to *S. coelicolor*. To verify this hypothesis, microwave digestion and ICP-MS were used to determine the content of copper in *S. coelicolor* cells when exposed to CuO NPs of 40 nm. After cultivation in each of the two media after 4 h concentrations of Cu in mycelium was the greatest when exposed to 40 mg/L of CuO NPs (Fig. 5). The mass of

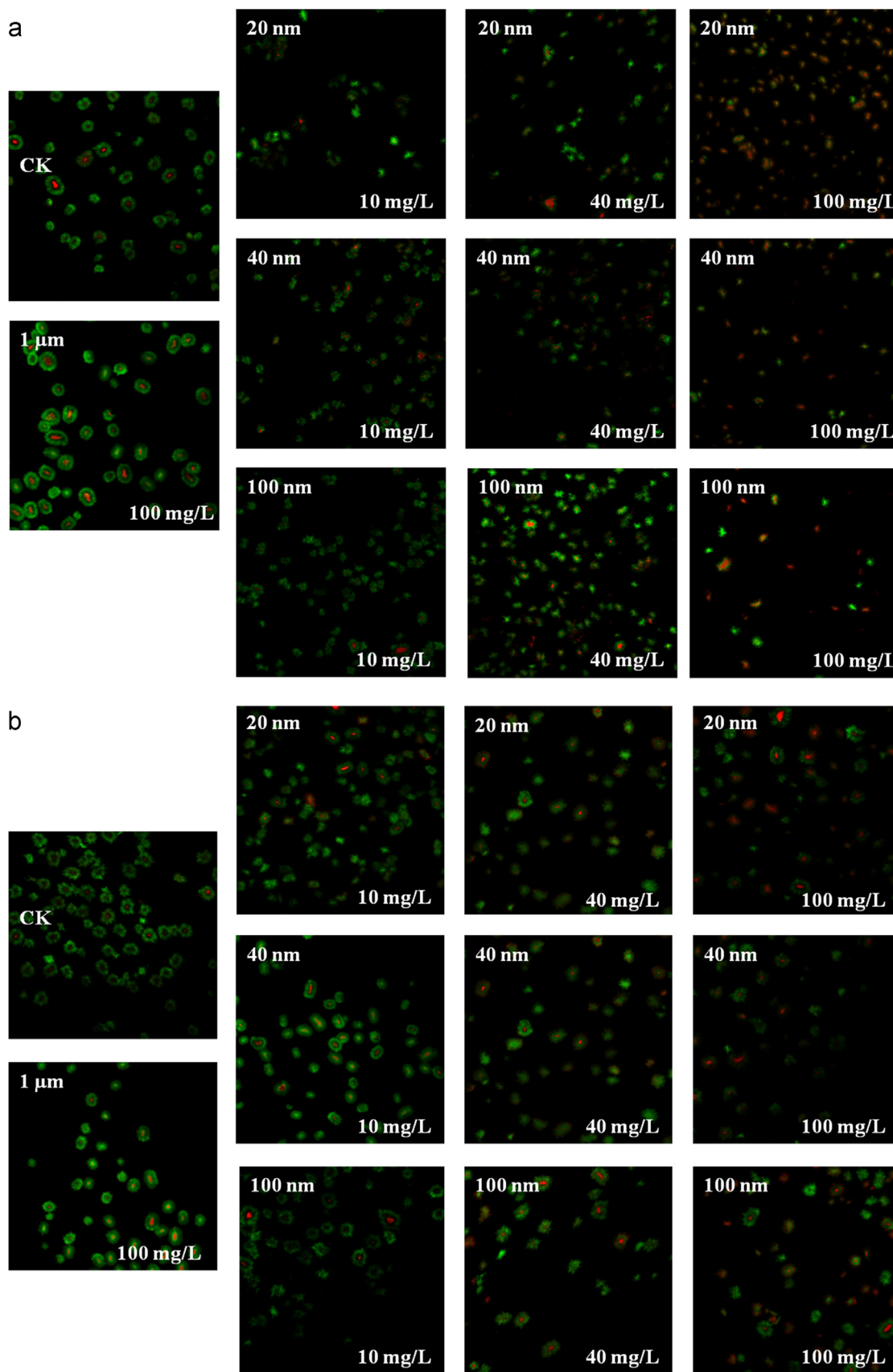


Fig. 4. The CLSM images of *S. coelicolor* M145 incubated with different size and concentration of CuO particles treatment in two media for 4 h: (a) in 0.9% NaCl, (b) in TSBY medium (CK mean the control without any particles). Cells were dyed with SYTO 9 (staining green, means living cell) and PI (staining red, means dead cell) before CLSM observation. All stained samples were imaged at comparable cell concentrations. The scale of each image was 3.9 mm × 3.9 mm, objective amplification was 10×, and the setting was consistent among images and exposure conditions.

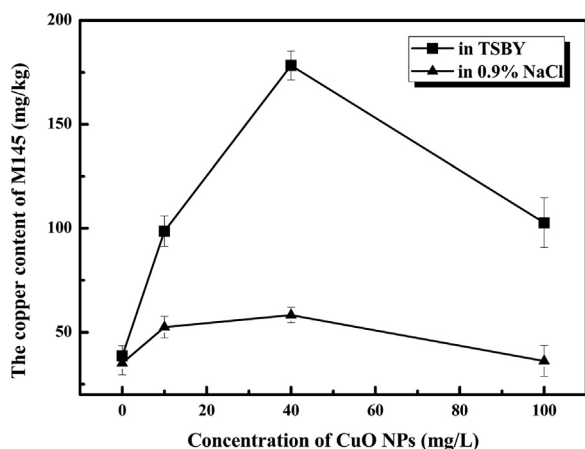


Fig. 5. Intracellular copper content of M145 in the two medium after shaking for 4 h. Error bar represent standard deviation (n = 3).

Cu in *S. coelicolor* cells cultured in TSBY medium (178.3 mg/kg) was greater than that in 0.9% NaCl solution (57.6 mg/kg). This indicated that in TSBY medium, a greater mass of Cu entered the mycelium, which caused toxicity to *S. coelicolor*, while in 0.9% NaCl solution, only a small amount of copper entered the mycelium, and most of the damage to membranes was caused by NPs outside the bacteria. When exposed to 100 mg/L CuO NPs, most bacteria were dead, which could not transform Cu²⁺ into the cell, and membranes were broken, which resulted in outflow of cytoplasm, so that concentrations of Cu in mycelium was less.

In order to determine whether Cu²⁺ or solid CuO NPs were the main factor contributing to toxic potencies of CuO NPs to *S. coelicolor* in these two media, the dissolved Cu²⁺ in different size CuO NPs was measured in the two media after shaking for 4 h. Regardless of whether NPs or BPs were used, solubility of Cu²⁺ was nearly zero in 0.9% NaCl (Table 1). While in TSBY medium, the concentration of Cu²⁺ was much greater and proportional to concentrations of NPs. When the concentration of CuO NPs was 100 mg/L, approximately 80% of total Cu was released into the medium as Cu²⁺. Also, there was no significant difference in release of Cu²⁺ (p > 0.05) among various sizes of NPs. These findings were inconsistent with those reported previously (Zhao et al., 2013).

To further verify that in TSBY medium, toxicity caused by Cu²⁺, mortality and concentrations of ROS caused to *S. coelicolor* by either CuO NPs or copper chloride (CuCl₂) with equivalent total concentrations of Cu²⁺ were investigated. Because there were no statistically significant differences in toxicity of CuO NPs among various particle sizes to M145 in TSBY medium, 40 nm CuO was chosen for further confirming whether the toxic effect was from the nano effect or the toxicity of Cu. Exposure to CuCl₂ reduced survival and viability (Fig. 6a), and resulted in greater concentrations of ROS (Fig. 6b) compared to the same parameters observed in *S. coelicolor* exposed to solid CuO NPs. The supernatant of the suspension of CuO NPs was used after shaking for 4 h and centrifugation to determine toxicity of the supernatant which contained Cu²⁺ in the absence of CuO NPs. Viability

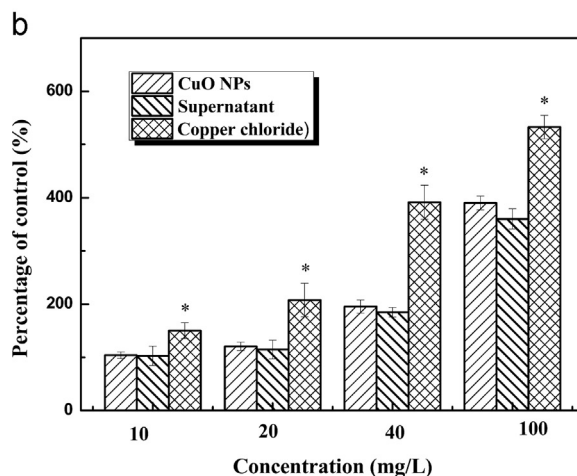
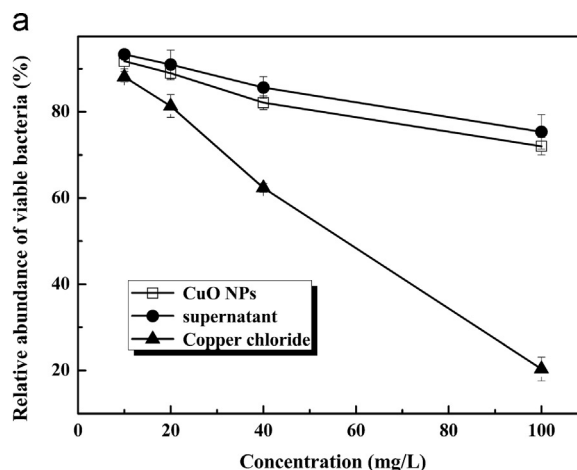


Fig. 6. Viability (a) and ROS level (b) of M145 exposed to different concentration CuO NPs, the supernatant of nano CuO, and copper chloride solution with the same concentration of copper ions in TSBY medium. * indicates that the treatment is significantly different (p < 0.05) from the treatment of CuO NPs of the same concentration. Error bar represent standard deviation (n = 3).

of *S. coelicolor* in the supernatant was almost the same with that of the CuO NPs, but greater than that of CuCl₂ alone. When exposed to 100 mg/L CuO NPs, viability of *S. coelicolor* was 72%, compared to 75% in the supernatant, while viability in the solution of CuCl₂ alone was 20%. Trends for concentrations of ROS were similar at each concentration. Concentrations of ROS in *S. coelicolor* exposed to the supernatant was almost the same as or slightly less than that of *S. coelicolor* exposed to CuO NPs, but the concentration of ROS in *S. coelicolor* exposed to CuCl₂ was greater. The results indicated that Cu²⁺ released from CuO NPs and with that in CuCl₂ might not be the same form. Maybe something in organic-rich medium reduce availability and thus toxic potency of Cu²⁺ reduced, a phenomenon that has been hypothesized previously (Gunawan et al., 2011). Due to high affinity of

Table 1

Solubilities of Cu²⁺ in various sizes (20 nm, 40 nm, 80 nm, 100 nm, 1 μm) and different concentration (10 mg/L, 40 mg/L and 100 mg/L) CuO NPs in 0.9% NaCl or TSBY medium.

	In 0.9% NaCl (mg/L)			In TSBY medium (mg/L)		
	10 mg/L	40 mg/L	100 mg/L	10 mg/L	40 mg/L	100 mg/L
20 nm	0.21 ± 0.03	0.32 ± 0.03	0.88 ± 0.03	4.02 ± 0.52	16.97 ± 1.58	64.63 ± 3.28
40 nm	0.18 ± 0.02	0.45 ± 0.09	0.92 ± 0.11	4.11 ± 0.36	16.15 ± 0.24	62.32 ± 2.03
80 nm	0.19 ± 0.01	0.38 ± 0.04	0.82 ± 0.28	3.98 ± 0.32	15.96 ± 0.81	60.45 ± 4.22
100 nm	0.17 ± 0.02	0.29 ± 0.06	0.79 ± 0.11	4.09 ± 0.27	15.65 ± 0.59	60.86 ± 3.59
1 μm	0.11 ± 0.04	0.28 ± 0.04	0.45 ± 0.09	0.49 ± 0.11	0.92 ± 0.26	1.12 ± 0.46

side chains of amino acids such as histidine, cysteine, and lysine, Cu^{2+} could form metal-ligand complexes that might decrease the activity of Cu^{2+} and thus result in lesser toxic potency to *S. coelicolor*.

4. Conclusions

To the knowledge of the authors, this is the first time that *Streptomyces* was exposed to CuO NPs. Different from more common bacteria, *Streptomyces* can form mycelial pellets that might be more easily affected by NPs. While the concentrations that caused adverse effects were relatively great compared to what would be expected to occur in the environment, the results of the study do provide insight into likely mechanisms of effects and can be used in assessments of risks to bacteria. In particular, these results have relevance to situations where the CuO NPs are used in treatment of wastewater. Compared with CuO NPs, toxicity of micrometer-sized CuO was deemed to be trivial. In 0.9% NaCl, solid particles were primary cause of toxicity, and toxicities of CuO NPs varied among sizes. In organic-rich TSBY medium, there was no significant difference in toxicity of various sizes of CuO NPs. While about 80% of Cu was in the form of Cu^{2+} , since some Cu still existed in the form of particles, it resulted in a slight difference in ROS in cells exposed to various sizes of particles. Though toxicity of CuO NPs was in part due to release of Cu^{2+} , the effect was less than that of added copper salts. This was due to the fact that the released Cu^{2+} formed complexes with organics. When toxicity of CuO NPs was compared between the two media, in TSBY medium, Cu^{2+} entered cells through membranes and then killed cells, so the size of the mycelium did not change although some of the bacteria died. While in 0.9% NaCl, solid particles destroyed cell membranes of *Streptomyces*, then killed the cells, which resulted in smaller pellets, smaller as shown by confocal laser scanning microscopy.

Acknowledgements

This work was supported by (1) National Natural Science Foundation of China [41473070], (2) Tianjin S&T Program [17PTGCCX00240], (3) Subproject of National Science and Technology Major Project [2015ZX07203-011-06], and (4) 111 program, Ministry of Education, China [T2017002]. Prof. Giesy was supported by the "High Level Foreign Experts" program [#GDT20143200016] funded by the State Administration of Foreign Experts Affairs, the PR China to Nanjing University and the Einstein Professor Program of the Chinese Academy of Sciences. He was also supported by the Canada Research Chair Program and a Distinguished Visiting Professorship in the School of Biological Sciences of the University of Hong Kong.

Declarations of interest

None.

Appendix A. Supplementary material

Supplementary data associated with this article can be found in the online version at <http://dx.doi.org/10.1016/j.ecoenv.2018.04.007>.

References

Aprile, C., Gobechiya, E., Martens, J.A., Pescarmona, P.P., 2010. New mesoporous composites of gallia nanoparticles: high-throughput synthesis and catalytic application. *Chem. Commun.* 46, 7712–7714.

Aruoja, V., Dubourguier, H.C., Kasemets, K., Kahru, A., 2009. Toxicity of nanoparticles of CuO, ZnO and TiO₂ to microalgae *Pseudokirchneriella subcapitata*. *Sci. Total Environ.* 407, 1461–1468.

Baek, Y.W., An, Y.J., 2011. Microbial toxicity of metal oxide nanoparticles (CuO, NiO, ZnO, and Sb₂O₃) to *Escherichia coli*, *Bacillus subtilis*, and *Streptococcus aureus*. *Sci. Total Environ.* 409, 1603–1608.

Balazs, A.C., Emrick, T., Russell, T.P., 2006. Nanoparticle polymer composites: where two small worlds meet. *Science* 314, 1107–1110.

Ben-Moshe, T., Dror, I., Berkowitz, B., 2009. Oxidation of organic pollutants in aqueous solutions by nanosized copper oxide catalysts. *Appl. Catal. B* 85, 207–211.

Bentley, S.D., Chater, K.F., Cerdeno-Tarraga, A.M., Challis, G.L., Thomson, N.R., James, K.D., Harris, D.E., Quail, M.A., Kieser, H., Harper, D., Bateman, A., Brown, S., Chandra, G., Chen, C.W., Collins, M., Cronin, A., Fraser, A., Goble, A., Hidalgo, J., Hornsby, T., Howarth, S., Huang, C.H., Kieser, T., Larke, L., Murphy, L., Oliver, K., O'Neil, S., Rabinowitz, E., Rajandream, M.A., Rutherford, K., Rutter, S., Seeger, K., Saunders, D., Sharp, S., Squares, R., Squares, S., Taylor, K., Warren, T., Wietzorrek, A., Woodward, J., Barrell, B.G., Parkhill, J., Hopwood, D.A., 2002. Complete genome sequence of the model actinomycete *Streptomyces coelicolor* A3(2). *Nature* 417, 141–147.

Bhatia, S.K., Lee, B.R., Sathyanarayanan, G., Song, H.S., Kim, J., Jeon, J.M., 2016. Medium engineering for enhanced production of undecylprodigiosin antibiotic in *streptomyces coelicolor*, using oil palm biomass hydrolysate as a carbon source. *Bioresour. Technol.* 217, 141–149.

Bibb, M.J., 2005. Regulation of secondary metabolism in *streptomyces*. *Curr. Opin. Microbiol.* 8, 208–215.

Binh, C.T., Tong, T., Gaillard, J.F., 2014. Acute effects of TiO₂ nanomaterials on the viability and taxonomic composition of aquatic bacterial communities assessed via high-throughput screening and next generation sequencing. *PLoS One* 9, e106280.

Borodina, I., Siebring, J., Zhang, J., Smith, C.P., van Keulen, G., Dijkhuizen, L., Nielsen, J., 2008. Antibiotic overproduction in *Streptomyces coelicolor* A3(2) mediated by phosphofructokinase deletion. *J. Biol. Chem.* 283 (37), 25186–25199.

Chu, T.T.B., Peterson, C.G., Tong, T., Gray, K.A., Gaillard, J.F., Kelly, J.J., 2015. Comparing acute effects of a nano-TiO₂ pigment on cosmopolitan freshwater phototrophic microbes using high-throughput screening. *PLoS One* 10 (4), e0125613.

Delgado, K., Quijada, R., Palma, R., 2011. Polypropylene with embedded copper metal or copper oxide nanoparticles as a novel plastic antimicrobial agent. *Lett. Appl. Microbiol.* 53 (1), 50–54.

Dinesh, R., Anandaraj, M., Srinivasan, V., Hamza, S., 2012. Engineered nanoparticles in the soil and their potential implications to microbial activity. *Geoderma* 173–174, 19–27.

Eduok, S., Martin, B., Nocker, A., Villa, R., Jefferson, B., Coulon, F., 2013. Evaluation of engineered nanoparticle toxic effect on wastewater microorganisms: current status and challenges. *Ecotoxicol. Environ. Saf.* 95, 1–9.

Gunawan, C., Teoh, W.Y., Marquis, C.P., 2011. Cytotoxic origin of copper(II) oxide nanoparticles: comparative studies with micron-sized particles, leachate, and metal salts. *ACS Nano* 5 (9), 7214–7225.

Heinlaan, M., Ivask, A., Blinova, I., 2008. Toxicity of nanosized and bulk ZnO, CuO and TiO₂ to bacteria *Vibrio fischeri* and crustaceans *Daphnia magna* and *Thamnocephalus platyurus*. *Chemosphere* 71, 1308–1316.

Hesketh, A., Chen, W.J., Ryding, J., 2007. The global role of ppGpp synthesis in morphological differentiation and antibiotic production in *Streptomyces coelicolor* A3(2). *Genome Biol.* 8 (8), R161.

Horie, M., Kato, H., Fujita, K., Endoh, S., Iwashita, H., 2012. In vitro evaluation of cellular response induced by manufactured nanoparticles. *Chem. Res. Toxicol.* 25 (3), 605–619.

Huang, B., Liu, N., Rong, X., Ruan, J., Huang, Y., 2015. Effects of simulated microgravity and spaceflight on morphological differentiation and secondary metabolism of *Streptomyces coelicolor* A3(2). *Appl. Microbiol. Biotechnol.* 99 (10), 4409–4422.

Jin, X., Li, M., Wang, J., Marambiojones, C., Peng, F., Huang, X., 2010. High-throughput screening of silver nanoparticle stability and bacterial inactivation in aquatic media: influence of specific ions. *Environ. Sci. Technol.* 44 (19), 7321–7328.

Kang, S., Herzberg, M., Rodrigues, D.F., Elimelech, M., 2008. Antibacterial effects of carbon nanotubes: size does matter!. *Langmuir* 24, 6409–6413.

Kim, M., Yi, J.S., Lakshmanan, M., Lee, D.Y., Kim, B.G., 2016. Transcriptomics-based strain optimization tool for designing secondary metabolite overproducing strains of *Streptomyces coelicolor*. *Biotechnol. Bioeng.* 113 (3), 651–660.

Lee, J., Mahendra, S., Alvarez, P.J.J., 2010. Nanomaterials in the construction industry: a review of their applications and environmental health and safety considerations. *ACS Nano* 4, 3580–3590.

Li, J., Zhou, H., Wang, J., Wang, D., Shen, R., Zhang, X., Jin, P., Liu, X., 2016. Oxidative stress-mediated selective antimicrobial ability of nano-VO₂ against Gram-positive bacteria for environmental and biomedical applications. *Nanoscale* 8 (23), 11907–11923.

Mohmand, J., Fasola, M., Alamdar, A., Mustafad, I., Ali, N., Liu, L., Peng, S., Shen, H., 2015. Human exposure to toxic metals via contaminated dust: bio-accumulation trends and their potential risk estimation. *Chemosphere* 132, 142–151.

Napierska, D., Rabolli, V., Thomassen, L.C., Dinsdale, D., Princen, C., Gonzalez, L., 2012. Oxidative stress induced by pure and iron-doped amorphous silica nanoparticles in subtoxic conditions. *Chem. Res. Toxicol.* 25 (4), 828–837.

Rajesh, T., Song, E., Kim, J.N., Lee, B.R., Kim, E.J., Park, S.H., 2012. Inactivation of phosphomannose isomerase gene abolishes sporulation and antibiotic production in *streptomyces coelicolor*. *Appl. Microbiol. Biotechnol.* 93 (4), 1685–1693.

Robichaud, C.O., Uyar, A.E., Darby, M.R., Zuckler, L.G., Wiesner, M.R., 2009. Estimates of upper bounds and trends in nano-TiO₂ production as a basis for exposure assessment. *Environ. Sci. Technol.* 43, 4227–4233.

Schaumann, G.E., Philippe, A., Bundschuh, M., Metrevelia, G., Klitzke, S., Rakcheev, D., Grün, A., Kumahor, S.K., Kühn, M., Baumann, T., Lang, F., Manz, W., Schulz, R., Vogel, H.J., 2015. Understanding the fate and biological effects of Ag and TiO₂ nanoparticles in the environment: the quest for advanced analytics and interdisciplinary concepts. *Sci. Total Environ.* 535, 3–19.

Sigle, S., Steblau, N., Wohlleben, W., 2016. Polydiglycosylphosphate transferase Pdta (SCO2578) of *Streptomyces coelicolor* A3(2) is crucial for proper sporulation and apical tip extension under stress conditions. *Appl. Environ. Microbiol.* 82 (18), 5661–5672.

- Tong, T., Shereef, A., Wu, J., 2013. Effects of material morphology on the phototoxicity of nano-TiO₂ to bacteria. *Environ. Sci. Technol.* 47 (21), 12486–12495.
- Vance, M.E., Kuiken, T., Vejerano, E.P., McGinnis, S.P., Hochella Jr., M.F., Rejeski, D., Hull, M.S., 2015. Nanotechnology in the real world: redeveloping the nanomaterial consumer products inventory. *Beilstein J. Nanotechnol.* 6, 1769–1780.
- Wang, Z., Zhao, J., Li, F., Gao, D., Xing, B., 2009. Adsorption and inhibition of acetylcholinesterase by different nanoparticles. *Chemosphere* 77, 67–73.
- Williamson, N.R., Fineran, P.C., Leeper, F.J., Salmond, G.P.C., 2006. The biosynthesis and regulation of bacterial prodiginines. *Nat. Rev. Microbiol.* 4, 887–899.
- [dataset] Woodrow Wilson Database. The Project on Emerging Nanotechnologies: Consumer Products Inventory. Woodrow Wilson International Centre for Scholars, Washington DC. <<http://www.nanoproduct.org/inventories/consumer/>>.
- Yang, Y.H., Fu, X.L., Li, L.Q., Zeng, Y., Li, C.Y., He, Y.N., 2012. Naphthomycins l–n, ansamycin antibiotics from *streptomyces* sp. *J. Nat. Prod.* 75 (7), 1409–1413.
- Zhao, J., Wang, Z., Dai, Y., 2013. Mitigation of CuO nanoparticle-induced bacterial membrane damage by dissolved organic matter. *Water Res.* 47 (12), 4169–4178.

Mechanisms of oxidative stress caused by CuO nanoparticles on membranes of the bacterium *Streptomyces coelicolor* M145

Xiaomei Liu¹, Jingchun Tang^{1*}, Lan Wang¹, John P. Giesy^{2,3}

¹Key Laboratory of Pollution Processes and Environmental Criteria (Ministry of Education),
Tianjin Engineering Center of Environmental Diagnosis and Contamination Remediation, College
of Environmental Science and Engineering, Nankai University, Tianjin 300350, China.

²Toxicology Centre, University of Saskatchewan, Saskatoon, Saskatchewan, Canada

³Department of Veterinary Biomedical Sciences, University of Saskatchewan, Saskatoon,
Saskatchewan, Canada

* Corresponding author: Jingchun Tang

Tel.: +86-22-83614117, Fax: +86-22-83614117

E-mail address: tangjch@nankai.edu.cn

Table S1. Characterization of different size of CuO in TSBY medium and 0.9% NaCl

	Concentration (mg/L)	0.9% NaCl			TSBY		
		pH	EC ($\mu\text{s}/\text{cm}$)	DLS (nm)	pH	EC (ms/cm)	DLS (nm)
20nm	10	6.53 ± 0.03	8.02 ± 0.05	268 ± 42.5	6.72 ± 0.02	6.21 ± 0.09	942 ± 78.2
	40	6.61 ± 0.08	7.86 ± 0.04		6.67 ± 0.01	6.23 ± 0.11	
	100	6.63 ± 0.01	6.97 ± 0.05		6.63 ± 0.02	6.25 ± 0.18	
40nm	10	6.32 ± 0.02	10.11 ± 0.04	328 ± 21.7	6.72 ± 0.04	6.23 ± 0.06	998 ± 59.6
	40	6.47 ± 0.05	9.27 ± 0.03		6.68 ± 0.02	6.25 ± 0.09	
	100	6.66 ± 0.09	8.10 ± 0.05		6.64 ± 0.05	6.27 ± 0.14	
80nm	10	6.42 ± 0.01	13.11 ± 0.03	368 ± 32.8	6.74 ± 0.05	6.38 ± 0.07	1021 ± 104
	40	6.53 ± 0.03	12.62 ± 0.06		6.69 ± 0.04	6.33 ± 0.08	
	100	6.76 ± 0.09	9.08 ± 0.21		6.60 ± 0.02	6.25 ± 0.13	
100nm	10	6.58 ± 0.04	13.42 ± 0.09	412 ± 52.7	6.72 ± 0.03	6.31 ± 0.12	1034 ± 88.5
	40	6.63 ± 0.04	12.88 ± 0.11		6.67 ± 0.01	6.27 ± 0.09	
	100	6.70 ± 0.03	10.35 ± 0.28		6.61 ± 0.08	6.23 ± 0.11	
1 μm	10	6.29 ± 0.04	8.32 ± 0.08	1329 ± 66.9	6.67 ± 0.09	6.21 ± 0.08	1720 ± 73
	40	6.33 ± 0.01	8.77 ± 0.11		6.67 ± 0.11	6.21 ± 0.21	
	100	6.36 ± 0.02	9.95 ± 0.06		6.64 ± 0.03	6.22 ± 0.05	

Table S2. The diameter of mycelia pellets under different size and different concentration CuO treatment in 0.9% NaCl and TSBY medium.

	In 0.9% NaCl (mm)			In TSBY medium (mm)		
	10 mg/L	40 mg/L	100 mg/L	10 mg/L	40 mg/L	100 mg/L
20 nm	0.15±0.03	0.12±0.03	0.11±0.02	0.26±0.05	0.28±0.05	0.28±0.05
40 nm	0.18±0.04	0.14±0.02	0.12±0.03	0.28±0.06	0.28±0.04	0.27±0.04
100 nm	0.17±0.02	0.15±0.02	0.14±0.03	0.32±0.03	0.29±0.05	0.29±0.04
1 μm	-----	-----	0.32±0.07	----	----	0.30±0.03

The control without any treatment was 0.34±0.03mm.

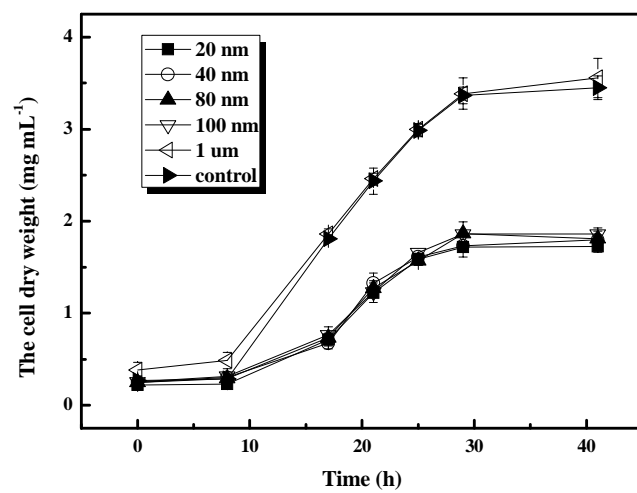


Figure S1. The change of growth curve after treated by different size of CuO at the concentration of 40 mg/L.

